

Characterizations of Periodic, Semi-Period, and Chaotic Motion of a Driven Pendulum

Guillermo Narvaez Paliza¹

¹*Martin A. Fisher School of Physics, Brandeis University, Waltham, MA 02453, USA*

(Dated: April 4, 2017)

For many deterministic systems we can exploit the laws of Physics to make an accurate estimation of the system state. For example, we can determine the speed of a falling ball at a given moment if we know the initial conditions and the time at which it was released. However, some systems that are completely constrained to the laws of Physics, seem to be unpredictable. We call this systems *chaotic*. Chaotic systems appear random because the intrinsic uncertainty of the measurement of the initial conditions grows quickly, specifically as an exponential function. As time increases, the uncertainty becomes large and predictions inaccurate. Here, we explore the non-linear, damped, driven pendulum, and explore the conditions under which the pendulum undergoes periodic, semi-periodic, and chaotic motion. We prove resonance and hysteresis in the driven pendulum and give several characterizations of motion that help us determine if a system is periodic or chaotic. Finally, we produce a bifurcation plot, which allows us to observe the phase transition of a system that goes back and forth, from periodic to chaotic.

INTRODUCTION

In the real world there exist many examples of deterministic systems that follow very well known physical laws, yet their motion seems to become unpredictable and random as time increases. These type of systems are truly deterministic and follow the well known laws of Physics, but whenever we predict the state of a system at a given moment we have also to account for an uncertainty. Moreover, in order to predict a system's future state, we need to have knowledge of the initial conditions, which is done through some measurement. In the real world, regardless of how accurately we measure things there will exist a certain uncertainty in the measurement. This initial uncertainty and the rate of change of the uncertainty determine if our predictions at a later time will be acceptable (within a certain uncertainty) or if the predictions will be completely inaccurate (making the system seem to have a random behavior).

Deterministic systems that seem random are sometimes called *chaotic*, since they have *deterministic chaotic dynamics*. The underlying reason why these systems seem *chaotic* is that the initial uncertainty inherited with the measurement of the initial conditions grows very fast, making the system appear random. Mathematically, on the one hand, for a non-chaotic system with some initial uncertainty Δx_0 , the uncertainty will grow linearly with time, allowing for reasonable predictions. At a later time the uncertainty would become $\Delta x(t) = \Delta x_0 \lambda t$. On the other hand, for a chaotic system with some initial uncertainty Δx_0 , the uncertainty grows as

$$\Delta x(t) = \Delta x_0 e^{\lambda t} \quad (1)$$

Systems whose initial uncertainty grows as defined by Equation 1 are referred as *unstable* systems. We define

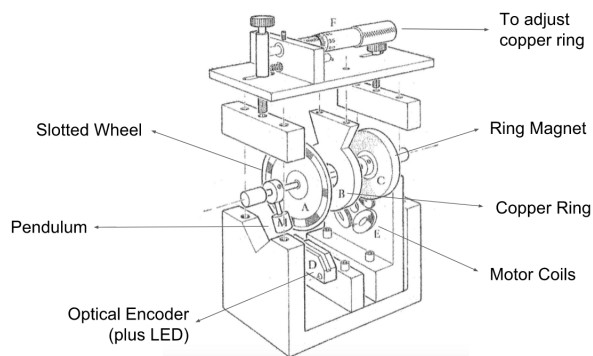


FIG. 1: Sinusoidally driven, damped, non-linear pendulum

chaotic systems as deterministic systems whose uncertainty of initial conditions grow exponentially with time. In other words, chaos arises when a system is unstable enough to present a random-like nature due to its sensitivity to initial conditions (Baker and Blackburn 2006). In contrast with chaotic systems, a physical system can also perform periodic or semi-periodic motion. For these cases, the motion of the system is confined to a given cycle, allowing us to predict the system's state at a later time. Simple Harmonic Oscillators undergo a periodic motion, while semi-periodic motion systems simply undergo more complex, yet closed cycles of motion.

We now explore the driven pendulum as an example of a system that can be both chaotic and non-chaotic. We explore the parameter space to find conditions under which the pendulum has a periodic, semi-periodic, or chaotic motion.

THE DRIVEN PENDULUM SYSTEM

In our experiments we use a sinusoidally driven, damped, non-linear pendulum as presented in Figure 1. The system consists of a mass attached to an axle (pendulum) to which a slotted wheel and a magnet ring are also attached. The pendulum, slotted wheel, and magnet are free to rotate around the axle with minimal friction. The slotted wheel moves in between an optical encoder, and with the help of an LED light, the computer software can determine the position of the pendulum and its rate of change (the velocity). The magnet ring is an octopole and it rotates near a static copper ring, generating Eddy currents in the copper ring, which consequently generate a damping torque on the axle's motion. The distance of the copper ring relative to the magnet can be varied with a micrometer screw, effectively changing the magnitude of the damping torque. Moreover, the magnet in addition to the motor coils enable us to provide a know torque to the axle.

THE DIMENSIONLESS EQUATION OF MOTION

For such a pendulum, the equation of motion becomes

$$I \frac{d^2\theta}{dt^2} + b \frac{d\theta}{dt} + mgd \sin \theta = \Upsilon \cos \omega_F t \quad (2)$$

where I is the moment of inertia, b is the friction parameter, mgd is the gravitational restoring torque, and Υ and ω_F are the amplitude of the drive and angular driving frequency, respectively. Now, aiming to reduce the number of parameters we attempt to find an equation with only dimensionless parameters. We define the dimensionless time as

$$\tau = \omega_0 t \quad (3)$$

where the natural frequency of the system is

$$\omega_0 = \sqrt{mgd/I} \quad (4)$$

This leads to a new equation of motion:

$$I \omega_0 \frac{d^2\theta}{d\tau^2} + b \omega_0 \frac{d\theta}{d\tau} + mgd \sin \theta = \Upsilon \cos \frac{\omega_F}{\omega_0} \tau \quad (5)$$

Dividing through by $I\omega_0^2$, we get:

$$\frac{d^2\theta}{d\tau^2} + \frac{b}{I\omega_0} \frac{d\theta}{d\tau} + \frac{mgd}{I\omega_0^2} \sin \theta = \frac{\Upsilon}{I\omega_0^2} \cos \frac{\omega_F}{\omega_0} \tau \quad (6)$$

and since $\omega_0 = \sqrt{mgd/I}$ we simplify and obtain

$$\frac{d^2\theta}{d\tau^2} + \frac{b}{I\omega_0} \frac{d\theta}{d\tau} + \sin \theta = \frac{\Upsilon}{I\omega_0^2} \cos \frac{\omega_F}{\omega_0} \tau \quad (7)$$

We can then define three dimensionless parameters Q , A , and ω_D as

$$Q = \omega_0 I / b \quad (8)$$

$$A = \Upsilon / (\omega_0^2 I) \quad (9)$$

$$\omega_D = \omega_F / \omega_0 \quad (10)$$

where Q is the inverse of the force of the damping, A is the strength of the forcing, and ω_D is drive frequency relative to the natural frequency. We can then derive the dimensionless equation of motion as

$$\frac{d^2\theta}{d\tau^2} + \frac{1}{Q} \frac{d\theta}{d\tau} + \sin \theta = A \cos \omega_D \tau \quad (11)$$

This equation, with the three dimensionless parameters, will determine the dynamics of the pendulum. This parameters will determine if a system is under periodic, semi-periodic, or chaotic motion.

CALIBRATION OF THE PENDULUM

In our driven pendulum, we can vary the voltage applied to damp the pendulum, the relative distance of the copper ring to the magnet, and the driving frequency with we provide an extra torque to the axle. By varying them, we are effectively determining Q (the friction parameter), A (the amplitude of the drive), and ω_D (the drive frequency relative to the natural frequency). However, in order to be able to modify these dimensionless parameters we need to find the natural frequency of the system, ω_0 , the damping of the system, b/I , and the normalized torque being applied to the system.

DETERMINING THE NATURAL FREQUENCY

When we apply a torque T to the system via an external motor, the equation of motion becomes,

$$I \frac{d^2\theta}{dt^2} + b \frac{d\theta}{dt} + mgr \sin \theta = T \quad (12)$$

In determining the natural frequency of the system we first turn the motor off to provide zero torque, and set the copper plate far enough from the magnet to avoid any dapming force. Hence, the equation of motion becomes

$$I \frac{d^2\theta}{dt^2} + mgr \sin \theta = 0 \quad (13)$$

Furthermore, we know that $\sin \theta \approx \theta$ for small angles, and that the frequency of oscillations is determined by $\omega_0 = \sqrt{mgr/I}$, which allows us to find analytically the period of oscillation of a pendulum as

$$P = P_0 \left[\frac{2}{\pi} K(k) \right] \quad (14)$$

where P_0 is the period in infinitesimally small oscillations, $k = \sin \theta_{max}/2$, and $K(k)$ is the complete elliptic integral of the first kind. We can then displace the pendulum and let it oscillate freely at small angles. We calculate the period of oscillations as functions of the maximum amplitude of oscillation. We can calculate the elliptic integral and easily determine the value of P_0 . We do so for several pairs of values of the period and maximum amplitude, determine P_0 and find the average P_0 . We find that

$$P_0 \approx 0.666 \text{ s} \quad (15)$$

and since the natural frequency is defined as $\omega_0 = 2\pi/P_0$, we get that the natural frequency of our pendulum is

$$\omega_0 \approx 9.46 \text{ rad/s} \quad (16)$$

However, since we can modulate the driving frequency in Hertz, we know by definition that $F = \omega_F/2\pi$, where F is the driving frequency (cycles/second). Moreover, we can express F as $F = \frac{1}{2\pi}\omega_0\omega_D$. Using the value obtained for $\omega_0 \approx 9.46$, we have that

$$F \approx 1.50\omega_D \quad (17)$$

DETERMINING THE DAMPING OF THE SYSTEM

The damping of the system will be modulated by the parameter Q , which is in turn determined by the distance of the copper ring relative to the magnet. In order to determine Q , we need to somehow measure the amount of damping as a function of the micrometer setting. Here, we do not apply any voltage to the system and record the motion of the pendulum oscillating at small angles for the micrometer screw with settings 4mm through 11mm, with a 1mm step. In this scenario, the equation of motion becomes

$$I \frac{d^2\theta}{dt^2} + b \frac{d\theta}{dt} + mgr\theta = 0 \quad (18)$$

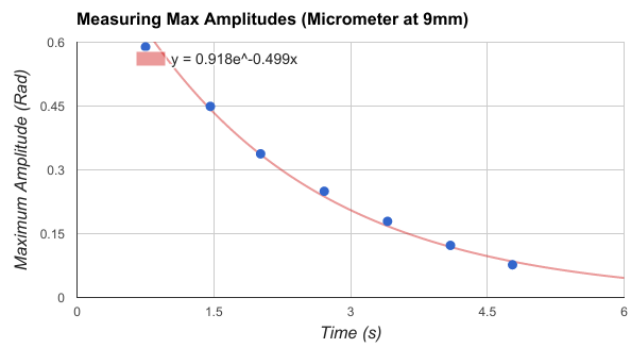


FIG. 2: Damping of oscillations for 9mm micrometer screw setting

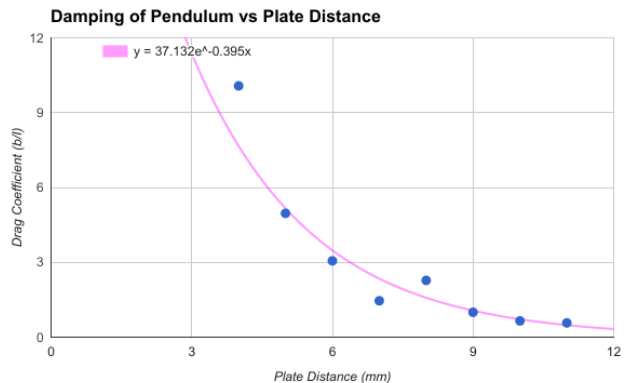


FIG. 3: b/I as a function of the micrometer setting

for which we can find the general solution for the amplitude of the oscillations as a function of time as

$$\theta = \theta_0 e^{-\alpha t} \cos \omega_1 t \quad (19)$$

where $\omega_1 = \omega_0^2 - \alpha^2$. Using this equation and the motion of the pendulum recorded for the different micrometer settings, we find α by fitting the data and extracting the coefficient of the exponent.

The resulting fitting for a 9mm micrometer setting can be observed in Figure 2, where $\alpha \approx 0.5$. Since $b/I = 2\alpha$, we can use all the resulting exponents (α) to plot b/I as a function of the micrometer setting (Figure 3), which can then be used to obtain Q for any of the settings. The resulting plot of Q as a function of the copper plate distance is shown in Figure 4.

DETERMINING THE NORMALIZED TORQUE

So far we have determined the natural frequency of the system and the damping of the system as a function of the micrometer screw setting. Now we find the relationship between the voltage that is being applied to

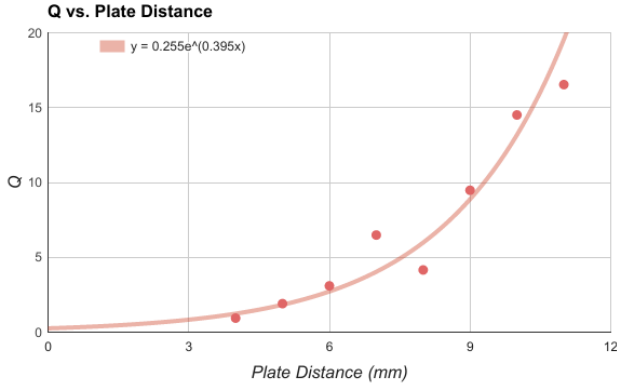


FIG. 4: Q as a function of the micrometer setting

the system and the effective torque being created on the axle. In order to do so, we position the pendulum on its side, such that the pendulum moves in a horizontal plane and neglecting any effect from gravity. The equation of motion becomes

$$I \frac{d^2\theta}{dt^2} + b \frac{d\theta}{dt} = T \quad (20)$$

We will then apply a series of voltages to the pendulum and let the pendulum reach equilibrium. When a terminal velocity is reached, the $\frac{d^2\theta}{dt^2}$ becomes zero, and the equation of motion becomes

$$T = b \left[\frac{d\theta}{dt} \right]_{term} \quad (21)$$

where T is a constant applied torque. Using the definition from equation 9, we find that

$$A = \frac{T}{\omega_0^2 I} = \frac{1}{\omega_0^2} \frac{b}{I} \left[\frac{d\theta}{dt} \right]_{term} \quad (22)$$

where the values of ω_0 and b/I have already been determined. From Figure 5, we can observe the linear dependency of the terminal velocity with respect to the applied voltage and model is as $\omega_{terminal} = \alpha V$, where $\omega_{terminal}$ is the terminal velocity, α is the constant of proportionality, and V is the voltage being applied. From the data, we find $\alpha \approx 8.50$, resulting in the last dimensionless parameter,

$$A = \frac{1}{\omega_0^2} \frac{b}{I} \alpha V \quad (23)$$

where all the coefficients in the right side of the equation are known.

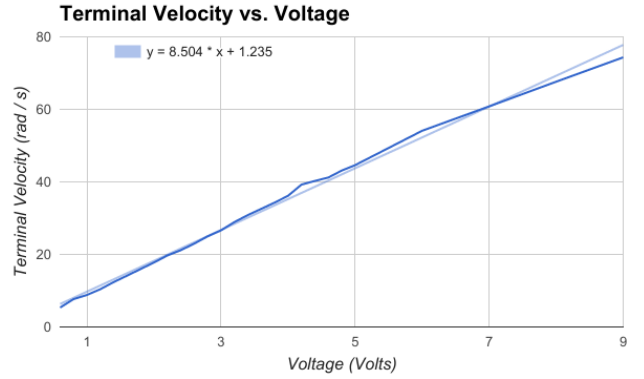


FIG. 5: Terminal velocity of pendulum as a function of applied voltage

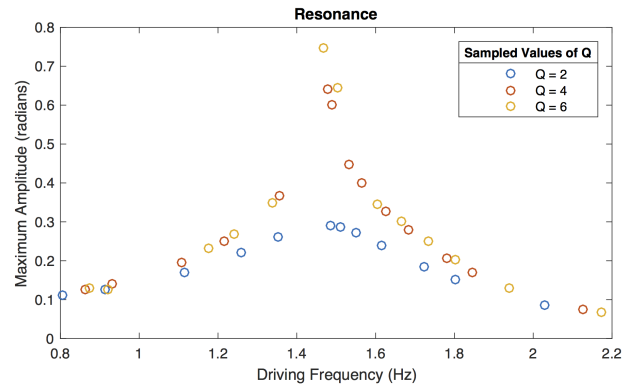


FIG. 6: Resonance curves for varying driving frequency and $Q = 2, 4, 6$

PROVING RESONANCE

Now that we have obtained the dimensionless equation of motion and the necessary calibration to tune the three dimensionless parameters, hence changing the dynamics of the system, we focus on exploring the parameter space to first demonstrate two important phenomena present in a driven pendulum, resonance and hysteresis, and then explore different characterizations of the dynamics of a driven pendulum.

In order to demonstrate resonance in the driven pendulum, we will observe the motion of the pendulum while oscillating at small amplitudes. We reduce the applied voltage until we obtain small oscillations and the pendulum becomes effectively a simple harmonic oscillator (SHO). This guarantees that chaotic motion will not occur. In order to prove that the system will reach maximum oscillation amplitudes when the system is driven at its natural frequency, we drive our pendulum from frequencies far below the natural frequency ω_0 to frequencies far above it.

The amplitude of oscillation as a function of the driving frequency is then recorded and plotted. This proce-

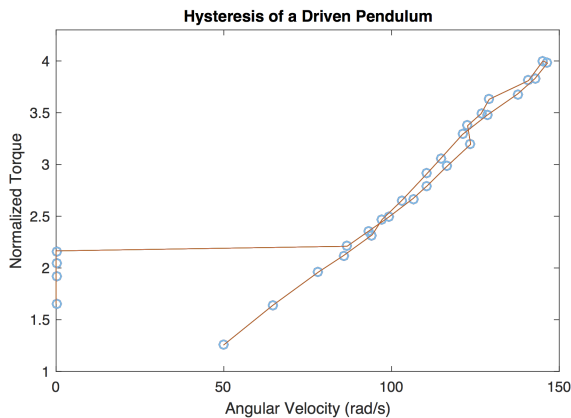


FIG. 7: Hysteresis in a driven pendulum present in the plot of the velocity as a function of the applied torque

ture is repeated for three different micrometer screw settings, such that the values of Q explored are 2, 4, and 6. From Figure 6 we can clearly see that the system presents maximum oscillations at $F \approx 1.5$ Hz, which agrees with $F \approx 1.50\omega_0$, for the natural frequency $\omega_0 \approx 0.96$ rad/s.

PROVING HYSTERESIS

Another important phenomenon that occurs in a driven pendulum is *hysteresis*. Some physical characteristics, such as the gravitational potential energy of two objects, is solely determined by the current state of the system – i.e. there exists only one possible value for the gravitational potential energy between two objects that are separated by a distance x . However, some systems, such as the driven pendulum present hysteresis, which means that the system’s phase depends of its kinetic path.

In our experiment, we explore the velocity of the pendulum for different values of the normalized torque. We start with the pendulum being still. We then start increasing the normalized torque in steps. At first we observe a slight increase in the pendulum’s angle. When the pendulum reaches 90 degrees it has reached the critical torque.

When we increase the torque by one more step, the pendulum begins to oscillate, and the velocity of the pendulum stops being zero. However, it is obvious that the velocity is not constant all around. In our data, we measure the average velocity $\langle d\theta/dt \rangle$ versus the normalized torque T/T_0 . From Figure 7 we observe that the pendulum remains static for increasing torque until a threshold is reached (the critical torque) and then the pendulum begins oscillating around the axle, resulting in a non-zero average angular velocity. However, when the pendulum has been set in motion, and we start decreasing the torque slowly, we reach the critical torque and the pen-

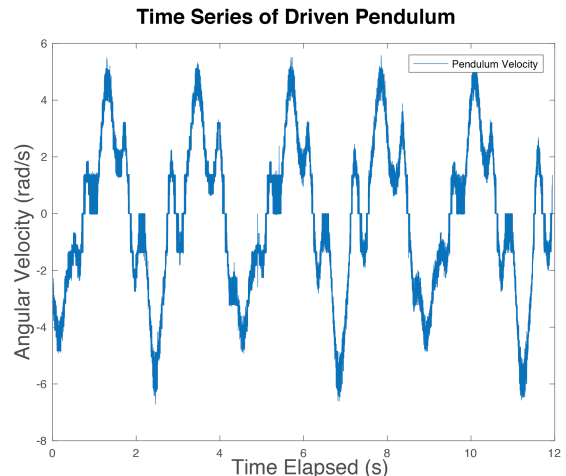


FIG. 8: Time series of a periodic motion ($Q = 2$, $A = 1.5$, $\omega_D = 0.5$)

dulum remains in motion. As we continue to decrease the torque, the pendulum still has a non-zero average angular velocity. This rupture between static and oscillating pendulums at equal applied torques is the proof of the presence of hysteresis in a driven pendulum, where the average velocity of the system depends on the kinetic history of the system.

RELEVANCE OF RESONANCE AND HYSTERESIS

Resonance and hysteresis are two interesting and useful physical phenomena that are worthy of study on their own. Here we have proven their presence in the driven pendulum. However, in our study of periodic, semi-periodic, and chaotic motion, resonance and hysteresis also provides us with some intuition to think about the problem. We observe an overlap of parameters, where in the case of resonance we can have a certain maximum amplitude of oscillation for several values of driving frequency and value Q . In the case of hysteresis, we observe that the system’s state is not uniquely determined by a set of parameters, but it is also dependent on the systems’ past. This properties of the driven pendulum lead to complex dynamics. We now explore different ways to characterize this complex dynamics.

CHARACTERIZATION OF MOTION

Our goal consists of finding different characterizations that help us find and understand under which sets of parameters the system goes periodic, semi-periodic, or complex motion. We now observe the pendulum under four different sets of values for the dimensionless param-

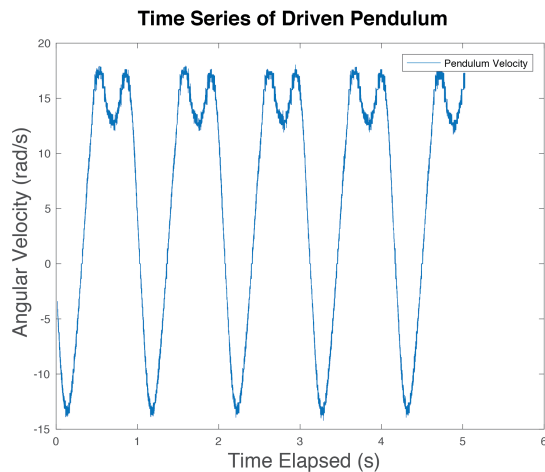


FIG. 9: Time series of a periodic motion ($Q = 4$, $A = 1.5$, $\omega_D = 1.0$)

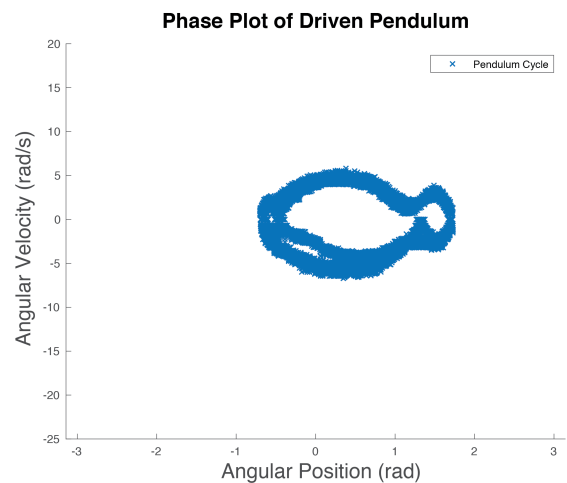


FIG. 12: Phase plot of a periodic motion ($Q = 2$, $A = 1.5$, $\omega_D = 0.5$)

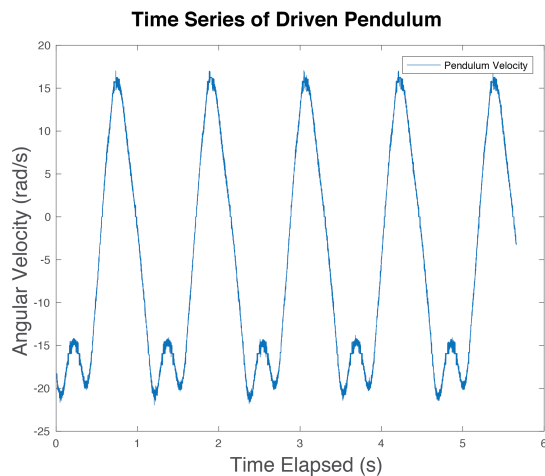


FIG. 10: Time series of a periodic motion ($Q = 2$, $A = 1.63$, $\omega_D = 0.9$)

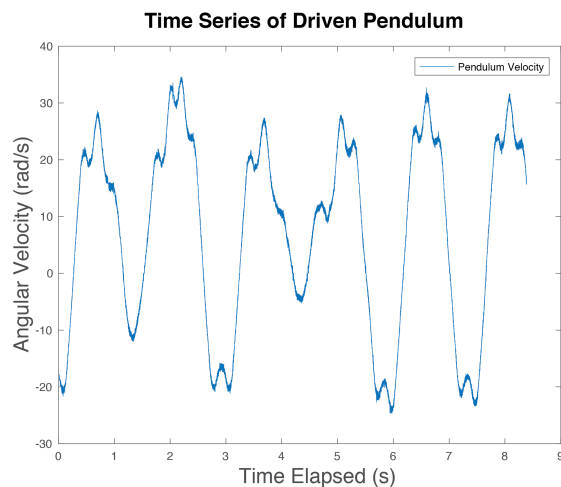


FIG. 11: Time series of a chaotic motion ($Q = 4$, $A = 1.5$, $\omega_D = 0.66$)

eters: $Q = 2$, $A = 1.5$, $\omega_D = 0.5$, $Q = 4$, $A = 1.5$, $\omega_D = 1.0$, $Q = 2$, $A = 1.63$, $\omega_D = 0.9$, $Q = 4$, $A = 1.5$, $\omega_D = 0.66$. The simplest way to approach this problem is through a time series. We can plot an observable as a function of time, and identify if the observable changes periodically – i.e. if the observable as a function of time follows a pattern.

From Figures 8 through 11, we can observe the results of measuring the velocity as a function of time, $\dot{\theta}(t)$. In Figures 8, 9, and 10, we observe a clear pattern in the time series indicating non-chaotic motion. However, it is clear from Figure 11 that the the velocity of the pendulum appears to change in a probabilistic-like fashion, indicating a chaotic system.

Perhaps an easier way of determining if a system is periodic, semi-periodic, or chaotic is looking at the phase plot where we plot $\dot{\theta}(\theta)$. In this plots we collect data for the pendulum's position and the pendulum's velocity for a given period of time.

The phase plots can be seen in Figures 12 through 15. Here we can appreciate the periodicity of the pendulum's motion (if any). The first observation is that Figures 12, 13, and 14 are constrained to a specific path, but Figure 15 never reaches the initial position, as expected for chaotic motion.

However, we can also differentiate between peiodic and semi-periodic motion. In Figure 12 we can see that there exists a unique cycle – the path does not intersect itself at any point. In Figures 13 and 14, however, there is a point where the path intersects itself, indicating a semi-periodic motion.

From the phase plots obtained, we see that at a certain angular position the possible angular velocities are contained within a finite set. This implies that regardless of how long has the system been oscillating, at that angular position the pendulum has a limited and unchanging set

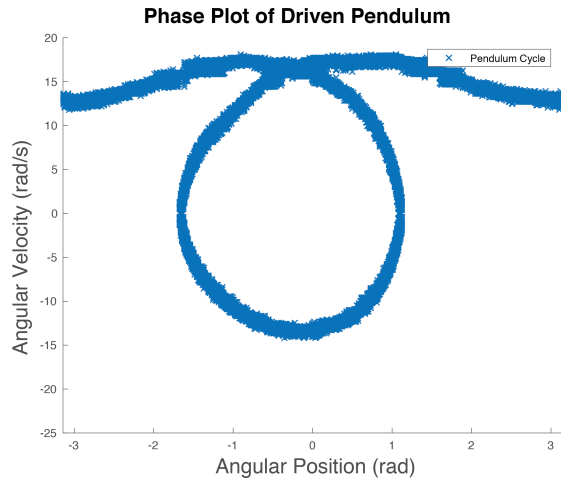


FIG. 13: Phase plot of a periodic motion ($Q = 4$, $A = 1.5$, $\omega_D = 1.0$)

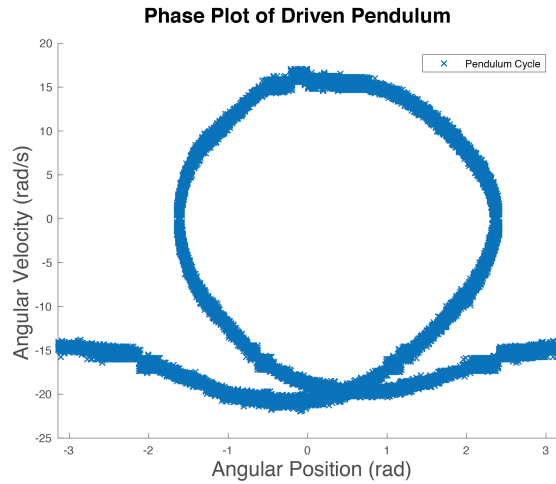


FIG. 14: Phase plot of a periodic motion ($Q = 2$, $A = 1.63$, $\omega_D = 0.9$)

of angular velocities. In order to characterize the motion of a driven pendulum, we use Poincare plots. Here, we measure the position and velocity of the pendulum constantly. We take a measurement once every period.

The plots presented in Figures 16 through 19 show the corresponding Poincare plots for the different motions. It is clear that Figures 16, 17, and 18, have a periodic motion since the plot shows that for every period (more specifically every measurement taken) there will be only one value for the velocity of the pendulum at the given angular position. In the case where multi-periodic motion is present, we would have two or more dots in the plot. In contrast, Figure 19 shows the Poincare plot for a chaotic motion. Here we observe that for every angular position there are many possible values for the angular velocity.

Another useful characterization of the motion of a

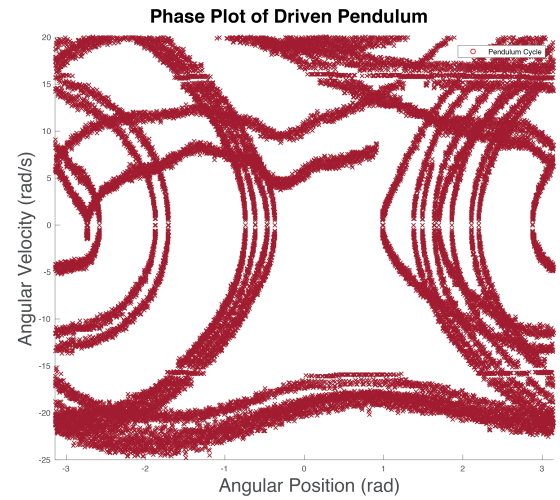


FIG. 15: Phase plot of a chaotic motion ($Q = 4$, $A = 1.5$, $\omega_D = 0.66$)

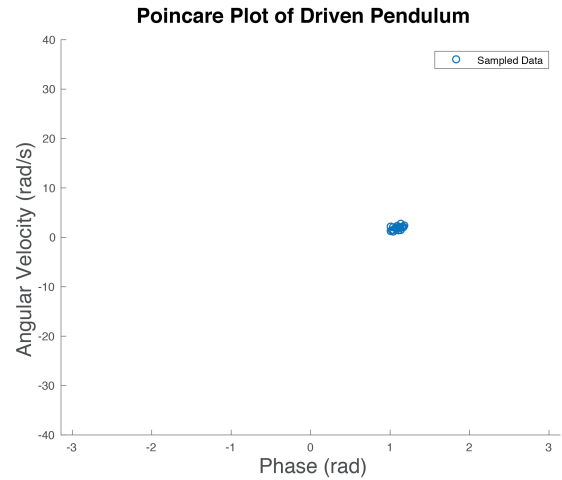


FIG. 16: Poincare plot of a periodic motion ($Q = 2$, $A = 1.5$, $\omega_D = 0.5$)

driven pendulum is the Fourier transform. For a discrete case, the Fourier transform can be expressed as

$$f(t) = a_0 + \sum_{n=1}^{\infty} a_n \cos(2\pi nx/L) + b_n \sin(2\pi nx/L) \quad (24)$$

where the coefficients a_n and b_n store information about the frequencies contained in f . In the continuous case, this Fourier transform becomes

$$f(t) = \int_{-\infty}^{\infty} A(\omega) e^{i\omega t} d\omega \quad (25)$$

where

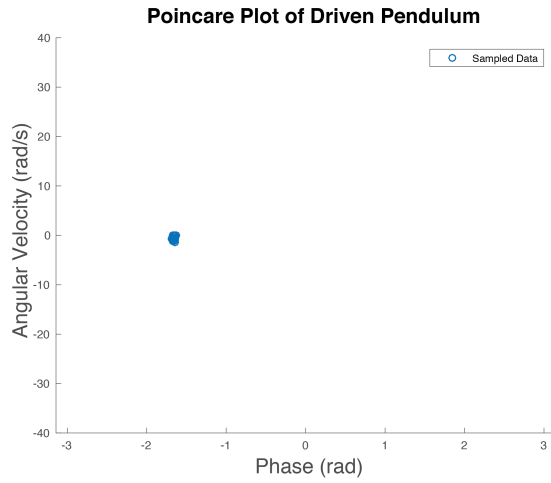


FIG. 17: Poincare plot of a periodic motion ($Q = 4$, $A = 1.5$, $\omega_D = 1.0$)

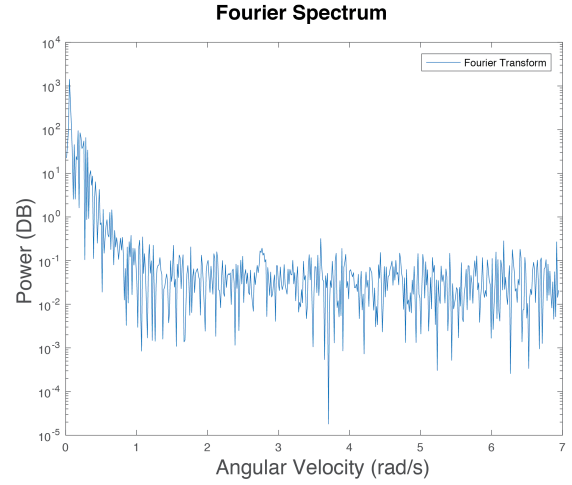


FIG. 20: Fourier transform of a periodic motion ($Q = 2$, $A = 1.5$, $\omega_D = 0.5$)

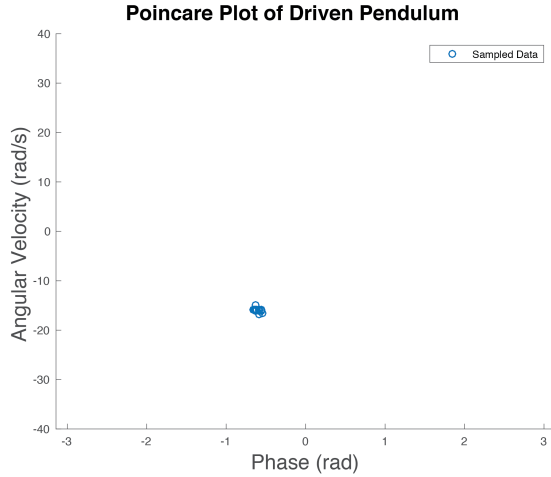


FIG. 18: Poincare plot of a periodic motion ($Q = 2$, $A = 1.63$, $\omega_D = 0.9$)

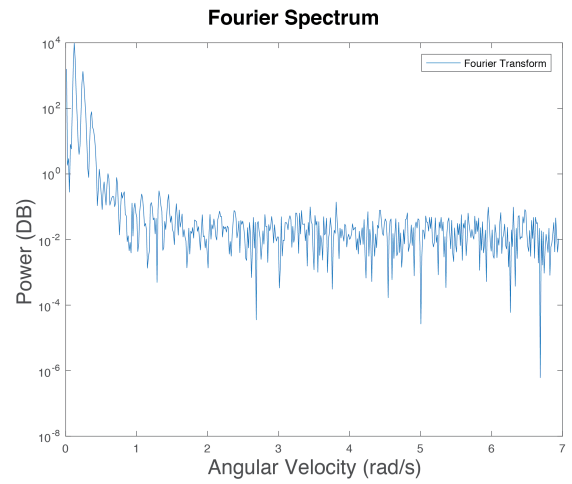


FIG. 21: Fourier transform of a periodic motion ($Q = 4$, $A = 1.5$, $\omega_D = 1.0$)

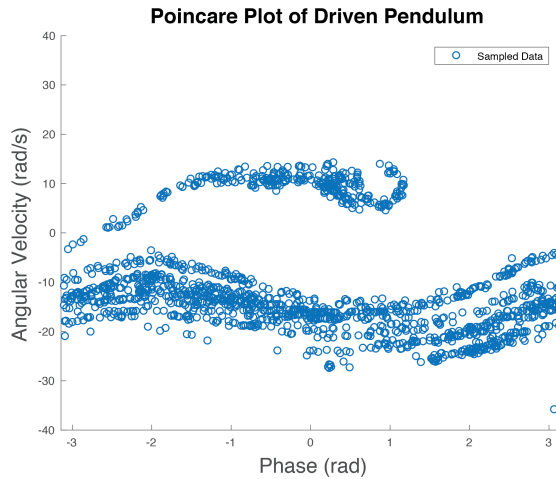


FIG. 19: Poincare plot of a chaotic motion ($Q = 4$, $A = 1.5$, $\omega_D = 0.66$)

$$A(\omega) = \int_{-\infty}^{\infty} f(t)e^{-i\omega t} dt \quad (26)$$

contains the information about the frequencies of oscillation. In Figures 20 through 23 we can see the fourier transforms of the different pendulum motions. We can observe that in the cases of periodic or semi-periodic motion, the periodicity of the system can be inferred from the pronounced peaks in the fourier transforms.

BIFURCATION PLOTS

We have shown several different ways in which the dynamics of the driven pendulum can be characterized. We now show how can we exploit this characterizations in

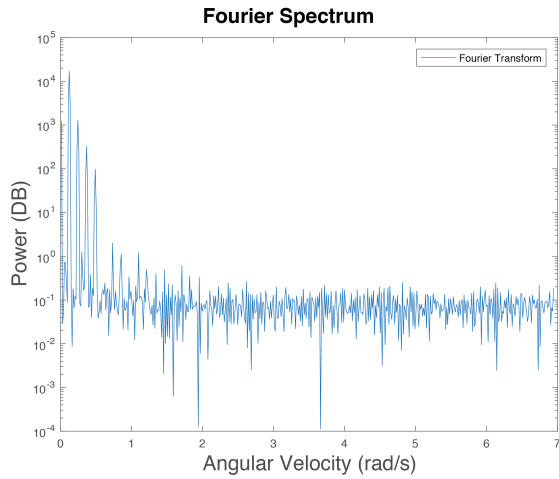


FIG. 22: Fourier transform of a periodic motion ($Q = 2$, $A = 1.63$, $\omega_D = 0.9$)

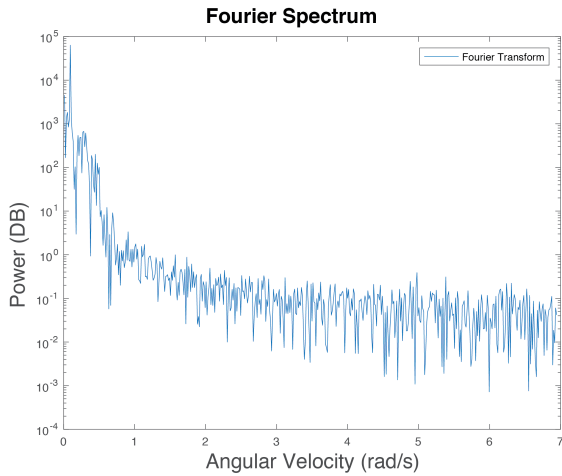


FIG. 23: Fourier transform of a chaotic motion ($Q = 4$, $A = 1.5$, $\omega_D = 0.66$)

order to determine under which conditions a driven pendulum exhibits periodic motion and under which others it exhibits chaotic motion, which is of great interest in our study. Using the Poincare plot we can extract the set of velocities that a specific system undergoes. We do so by extracting the vertical component (angular velocity) of all the data in the Poincare plot.

This is the basic idea of a bifurcation plot. Our dimensionless equation of motion contains three dimensionless parameters, which we can modify to determine the dynamics of the pendulum. We can hold two of these three parameters constant and modify the third one in order to see the phase transitions of the pendulum, going back and forth from periodic to chaotic motion.

Figure 24 shows the system for $Q = 4$, $A = 0.75$ and varying driving frequency. We slowly increase the driving frequency letting the pendulum reach an equilib-

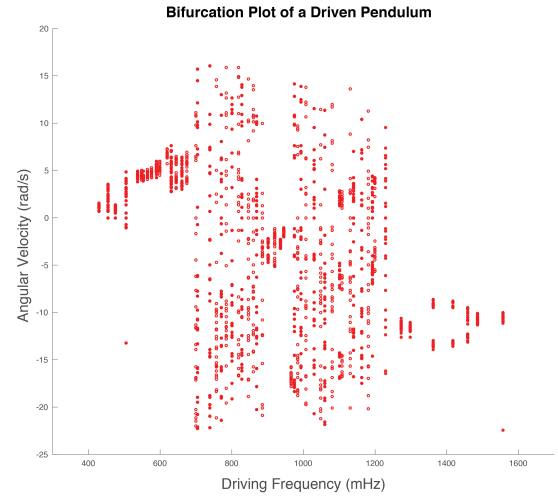


FIG. 24: Experimental bifurcation diagram ($Q = 4$, $A = 0.75$)

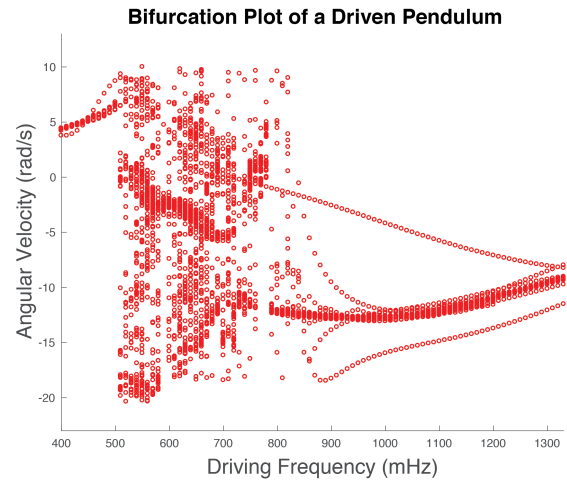


FIG. 25: Computational bifurcation diagram ($Q = 4$, $A = 0.75$)

rium state. We then collect data to produce a Poincare plot and extract all the vertical components (velocities) from the plot. We then plot the set of velocities for the given driving frequency. We repeat this process until we have spanned the wanted range. The result (Figure 24) show subsets of the parameter-space where the motion is periodic (sections of the bifurcation plot where we see connecting lines), and other subsets where the motion is chaotic (sections where the velocities are spread over most values of the angular velocity). Figure 25 show a computer simulation where the transition between periodic and chaotic becomes clearer, as the system does not go through a period of stabilization. This plots represent the mapping of the phase transitions between periodic and chaotic behavior.

CONCLUSIONS

We have seen that a non-linear, damped, driven pendulum is a complex system that presents deterministic behavior. However, we have shown that under certain conditions (specific combinations of the dimensionless parameters) the inherited uncertainty of the initial conditions grows exponentially, making the system unstable, which then results in the motion of the pendulum to appear probabilistic-like. When we observe this instability we call the system *chaotic*. We have shown the presence of resonance and hysteresis, and have explored the parameter space of the pendulum. Using the dimensionless equation of motion, we can easily adjust the pendulum to find periodic, semi-periodic, and chaotic motion.

We have shown how we can use different characterizations of the pendulum's dynamics to identify chaotic and non-chaotic systems. More importantly, we have generated a map that can be used to determine if the pendulum will undergo chaotic motion or not (the bifurcation plot). We present the results for a bifurcation plot for varying driving frequency to emphasize the perks of such a characterization of motion, but the study can be extended to explore different sets of parameters.

REFERENCES

1. Baker, G. & Blackburn, J. The pendulum a case study in physics (2006) Oxford University Press (Oxford, UK).